Earth and Planetary Science Letters 516 (2019) 156–163

Contents lists available at ScienceDirect

Earth and Planetary Science Letters

www.elsevier.com/locate/epsl

Equilibrium crystallization modeling of Venusian lava flows incorporating data with large geochemical uncertainties

Kyle T. Ashley *, Michael S. Ramsey

Department of Geology and Environmental Science, University of Pittsburgh, 4107 O'Hara Street, Pittsburgh, PA 15260, USA

ARTICLE INFO

Article history:
Received 23 August 2018
Received in revised form 8 March 2019
Accepted 27 March 2019
Available online xxxx
Editor: T.A. Mather

Keywords:
Venera 14
solidification
Monte Carlo method
apparent viscosity

ABSTRACT

Our understanding of the Venusian surface composition is limited to the *in-situ* bulk rock chemical analyses collected by the Vega and Venera missions. However, these analyses have exceedingly large analytical uncertainties – up to 50% by weight (1σ) for certain oxide components. In this study, we use the Venera 14 lander data and apply a Monte Carlo approach to assess how significant uncertainties affect modeling of lava solidification. Thermodynamic modeling of mineral-melt equilibria is conducted over 1,000 iterations of simulated bulk composition within the Gaussian probabilistic bounds of the reported analytical uncertainty along a cooling path from 1350 °C to 950 °C, with a fixed pressure of 90 bars. The results are used to calculate melt and apparent viscosity (η_{melt} and η_{app}, respectively). Despite the significant analytical uncertainty of the lander data, lava viscosity is tightly constrained. Mean log η_{melt} increases from 1.65 ± 0.46 Pa s at 1350 °C to 8.57 ± 1.42 Pa s at 950 °C (1σ). Log η_{app} is less well-defined due to increased scatter in crystal fraction with solidification, increasing to 17.7 ± 1.3 Pa s at 950 °C ($\gamma = 10^{-6}$ s^{-1}). A significant increase in η_{app} occurs between 1240 °C and 1080 °C due to a rapid increase in crystal mass fraction (Φ increases from ~0.05 at 1250 °C to 0.8 at ~1100 °C). Slow cooling through this 150 °C window must occur so as to not drastically increase lava viscosity and impede flow. These results show that despite limited geochemical data and large analytical uncertainties, reasonable constraints for the physical and chemical evolution of lava solidification can be obtained. Most of the Venusian surface is composed of volcanic plains and rises, containing abundant landforms characteristic of fluid basaltic lava. Our results provide new insights into the crystallization processes in Venusian lava flows, which are fundamental for understanding Venusian igneous processes, geodynamics, and resurfacing. This work provides a necessary framework for future thermorheological flow models to determine flow volume and effusion rates.

1. Introduction

Venus is the terrestrial planet most similar to Earth with respect to size, composition, and internal structure. Despite this, most of Venus' surface is composed of volcanic plains and rises (70–80%; Fegley, 2004; Hansen and Young, 2007), containing abundant landforms characteristic of fluid basaltic lava (Bruno and Taylor, 1995; Crumpler et al., 1997). There are no known meteorite samples from Venus, therefore our understanding of its surface composition is limited to the geochemical data collected by three lander missions sent by the former Soviet Union. Three landers (Venera 13, 14 and Vega 2) collected *in-situ* chemical analyses, however these analyses have exceedingly large analytical uncertainties – up to 50% by weight (1σ) for certain oxide components (Surkov et al., 1984, 1986). Our ability to understand the petrogenesis of the basaltic lavas that dominate the surface of Venus and unravel the geodynamics of the Venusian interior is dependent on these analyses; however, rarely are the effects of these uncertainties on the modeling approaches considered. Thermochemical models to predict crystallization sequences, which control the physical properties of the lava, requires knowledge of the bulk rock chemistry. Any effort to estimate effusion volumes and flow rates is dependent on this petrologic insight, which will provide better insight into Venusian igneous processes and resurfacing. This raises the question: Are the analytical uncertainties too large to compute meaningful results, or can probabilistic confidence envelopes be developed that present robust petrologic and rheologic constraints for Venusian volcanic processes?

In this paper, we use the Venera 14 lander data and apply a Monte Carlo approach to assess how these uncertainties affect thermodynamic modeling of lava solidification. Chemical analysis from the Venera 14 landing site was selected over the Vega 2 and

* Corresponding author.
E-mail address: ktashley@pitt.edu (K.T. Ashley).

https://doi.org/10.1016/j.epsl.2019.03.036
0012-821X/

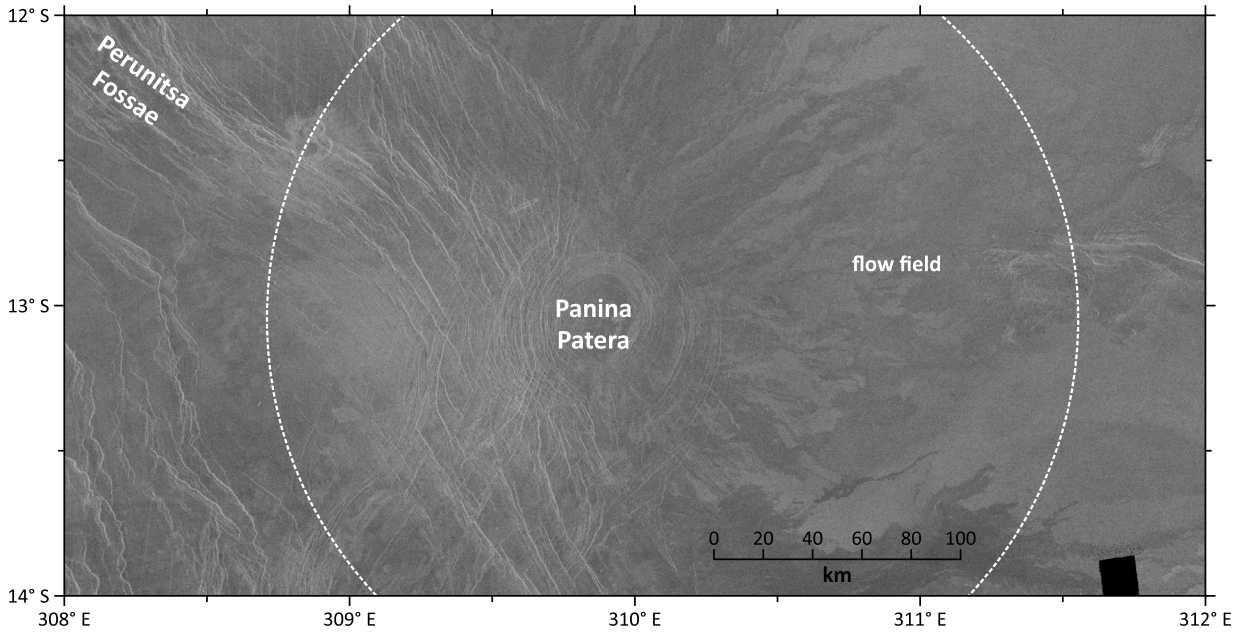

Fig. 1. Full resolution synthetic aperture radar (SAR) mosaic collected by the Magellan radar system showing landing region of Venera 14. The landing circle is shown for reference (dashed circle, centered at 13.05°S, 310.19°E). Smaller flows can be observed to the East of the caldera, which connects to a massive flow field extending >500 km to the East (Kargel et al., 1993, their Fig. 3).

Venera 13 whole rock analyses because the Vega 2 data have a low summed oxide total (~89.6 wt.%, Surkov et al., 1986), suggesting significant alteration and/or missing components (Grimm and Hess, 1997; Treiman, 2007). Similarly, lander photographs from Venera 13 revealed apparent chemical weathering and soil development (Surkov et al., 1984). The modeling results of the Venera 14 data are used to calculate the relative viscosity (η_r), which is the ratio between the system (melt and crystal) viscosity and the viscosity of the melt phase (η_{melt}). Apparent viscosity ($\eta_{app} = \eta_r \cdot \eta_{melt}$) is calculated for lava flows on Venus with decreasing temperature to constrain the rheologic evolution of the lava through crystallization. These calculations provide critical insight into conditions that control flow dynamics, and the results provide a framework for conducting future flow modeling based on well-tested terrestrial thermorheologic approaches to determine flow volumes and lava effusion rates.

2. Venus volcanism and local geology of the Venera 14 landing site

On Venus, atmospheric convection is suppressed and the radiation of heat from lava flows is reduced due to the hot dense CO_2-rich atmosphere, which has strong absorption regions in the infrared (Snyder, 2002). Consequently, lava takes significantly more time to cool than their equivalents on Earth, resulting in flows that can extend over a thousand kilometers. Warming of the Venusian surface occurs as a result of the CO_2-dominated atmosphere (~96.5%), producing ambient surface conditions of 462 °C and 92.1 bar at the mean planetary radius (6052 km; Seiff et al., 1986; Fegley et al., 1996). Conditions local to the Venera 14 landing site are 460 ± 2.3 °C and 90.4 ± 1.7 bars (Seiff et al., 1986). The surface also experiences exceptionally slow erosion and burial, which allows the preservation of features and structures for geologically long intervals (Basilevsky and McGill, 2007).

The Venera 14 landing site falls within a zone centered at 13.05°S latitude, 310.19° longitude on Navka Planitia, near the eastern flank of Phoebe Regio (Weitz and Basilevsky, 1993; Fig. 1). The landing occurred on/near the caldera of a ~75 km-wide shield volcano (Panina Patera), with tholeiitic basaltic rocks containing subhorizontal stratification (Surkov et al., 1984). Panina Patera is one of many conical shields in the Aleksota Mons shield field (Stofan et al., 2001; Malliband et al., 2017). Extensive rifting is present in the Perunitsa Fossae, which terminates at the Vostrukha Mons to the northwest and joins Panina Patera to the south. Ridge style volcanism has been identified in Khosedem Fossae to the west (Grindrod et al., 2010); NW-SE trending preferred orientation of vent alignment in the Aleksota Mons shield field suggests volcanism is associated with faulting in Perunitsa Patera (Malliband et al., 2017). Rift-related volcanism is supported by the presence of tholeiitic basalt, similar to MORB compositions on Earth (Gale et al., 2013; *Auxiliary Material*, Fig. S1), and by numerous lava flows emanating from rift fractures observed ~600 km south of the volcano (Weitz and Basilevsky, 1993). Flows emanating from the eastern slope of Panina Patera volcano edifice range from 10's to 100's of km in length. Volcanism is interpreted to be relatively young due to the series of concentric fractures centered on the volcano cross-cutting existing terrain, including small impact craters (Weitz and Basilevsky, 1993). Lobate planes proximal to the caldera coalesce into radial, fan-like patterns with no evidence of deformation; flows distal from the volcano contain networks of narrow wrinkle ridges that deformed mafic lavas by compressional forces (Abdrakhimov, 2001). Most of these deformed plains are extensively buried by more recent flows (Weitz and Basilevsky, 1993).

Previous petrologic studies of Venus have focused on melt production and petrogenesis of magma. Lee et al. (2009) determined depth and temperature of magma generation, using the Vega and Venera lander geochemical data. Assuming a Venusian mantle similar in composition to Earth (Lodders and Fegley, 1998), Lee et al. (2009) propose melting at 12–30 kbar and ~1350–1450 °C, with ~15 kbar and ~1400 °C proposed for the Venera 14 magma source. These results consider fractionation until a mantle source composition of Mg# = 0.9 was achieved, whereas unfractionated results predict melt generation at ~5 kbar and ~1250 °C for the Venera 14 geochemical data. Note that these calculations assume no ferric iron present (i.e., all iron is in the divalent form). Shellnutt (2016) estimated the mantle potential temperature associated with the Venera 14 volcanism to be ~1310–1440 °C and concluded the melt composition is consistent with a tensional rift

Table 1
Bulk rock geochemistry for Venera 14 compared to the mean of the simulated chemistries (pre- and post-culling).

	Measured		Simulated (pre-culling)		Simulated (post-culling)	
	wt.%	1σ	wt.%	1σ	wt.%	1σ
SiO_2	48.7	3.6	48.6	3.6	49.0	3.5
TiO_2	1.25	0.41	1.24	0.41	1.26	0.40
Al_2O_3	17.9	2.6	18.0	2.6	18.0	2.6
FeO	8.8	1.8	8.8	1.7	8.7	1.7
MnO	0.16	0.08	0.16	0.08	0.16	0.08
MgO	8.1	3.3	8.2	3.2	8.1	3.0
CaO	10.3	1.2	10.3	1.2	10.2	1.2
Na_2O	2.4[a]	0.4	2.4	0.4	2.4	0.4
K_2O	0.2	0.07	0.2	0.07	0.2	0.07

[a] Calculated value. Measured data from Surkov et al. (1984). Simulations included 1127 and 1000 iterations for pre-culling and post-culling, respectively.

system rather than a mantle-plume system, which would require anomalously high potential temperature (>1550 °C; e.g., Campbell, 2007; Herzberg et al., 2007; Herzberg and Gazel, 2009).

3. Methods

3.1. Handling large geochemical uncertainties

One of the largest challenges of thermodynamically modeling the solidification of Venusian lava flows is the large uncertainties on the reported surface chemistries. For the rock analyzed at the Venera 14 landing site (Surkov et al., 1984), major element oxide chemistry has 1σ uncertainty up to 50% of the measured oxide weight percent (Table 1). In contrast, laboratory geochemical measurements through techniques such as X-ray fluorescence typically result in measurements with uncertainty lower by a factor of 10 or more, typically <<1% (e.g., Magganas and Koutsovitis, 2015; S. Mertzman, Franklin and Marshall College, personal communications). Determination of the crystallization sequence, phase proportions, phase compositions, and other extensive variables through a Gibbs free energy (ΔG) minimization approach is dependent upon the bulk rock composition, and calculations assuming the measured chemistry without consideration for the large analytical uncertainty may lead to erroneous results.

In this paper, we use thermodynamic calculations to assess melt and apparent (crystal + melt) viscosity during lava solidification. Because propagation of the geochemical uncertainty cannot be completed in the 9-component system (SiO_2–TiO_2–Al_2O_3–FeO–MnO–MgO–CaO–Na_2O–K_2O) with many coupled degrees of freedom, we apply a Monte Carlo method of repeated random sampling for the bulk rock chemistry within the analytical uncertainty. For each oxide, a normal Gaussian continuous probability distribution curve is constructed, where the resultant 68.27% confidence interval (i.e., $\pm 1\sigma$) matches the reported analytical uncertainty by Surkov et al. (1984; Fig. 2a). A minimum sampling of 1,000 iterations is required because the mean oxide composition approaches the asymptote continuously within 0.1 wt.% at this level (Fig. 2b). Some simulated bulk rock chemistries resulted in calculations where there was no convergence on ΔG; these data points were culled and removed (see Section 3.2 for further discussion). A total of 1,121 iterations were conducted in this study to achieve 1,000 iterations after the culling process (see *Auxiliary Material* for all compositions used). The resultant mean and 1σ standard deviation is statistically indistinguishable to the measured geochemistry (Table 1). This allows for a comprehensive evaluation of the calculated thermodynamic and rheologic properties of the Venusian lavas, as well as an assessment of the impact of large analytical uncertainties on these results.

3.2. Thermodynamic and rheologic calculations for solidification of Venusian lava flows

Thermodynamic modeling of mineral-melt equilibria is completed in the program PELE v.8.01b (Bourdreau, 1999), which is based on the MELTS algorithms and database by Ghiorso (1985) and Ghiorso and Sack (1995). Calculations are iterated for the simulated bulk compositions (discussed above), assuming an anhydrous environment fixed to a fayalite-magnetite-quartz (FMQ) redox buffer. The assumption of an anhydrous melt is warranted given that most basaltic flows at elevations below ~2.4 km have radar properties indicative of anhydrous basalt (Fegley, 2004). In addition, high surface temperature and volcanic degassing leads to a dehydrated crust and gradual dehydration of the Venusian interior (Kaula, 1995; Mackwell et al., 1998), although differences in mantle volatile composition may also be the result of differences during planetary accretion, different thermal evolution, or due to the recycling of metamorphosed highlands (Hess and Head, 1990). For each simulated composition, the component weight percent oxides are entered into the PELE graphical user interface and the ferric iron content is computed for the FMQ redox state at the starting *P*–*T* conditions. The oxide totals are normalized to 100% and the model allowed to run from 1350 °C to 950 °C in 2 °C increments (fixed at 90 bars). Starting the modeled temperature at 1350 °C covers the eruptive temperature range (1240 °C to 1350 °C) modeled by Shellnutt (2016). A MATLAB script was written to handle data parsing, where data are extracted from the three output files (containing the calculated results for the solids, liquid and bulk systems) and stored into separate data files. The

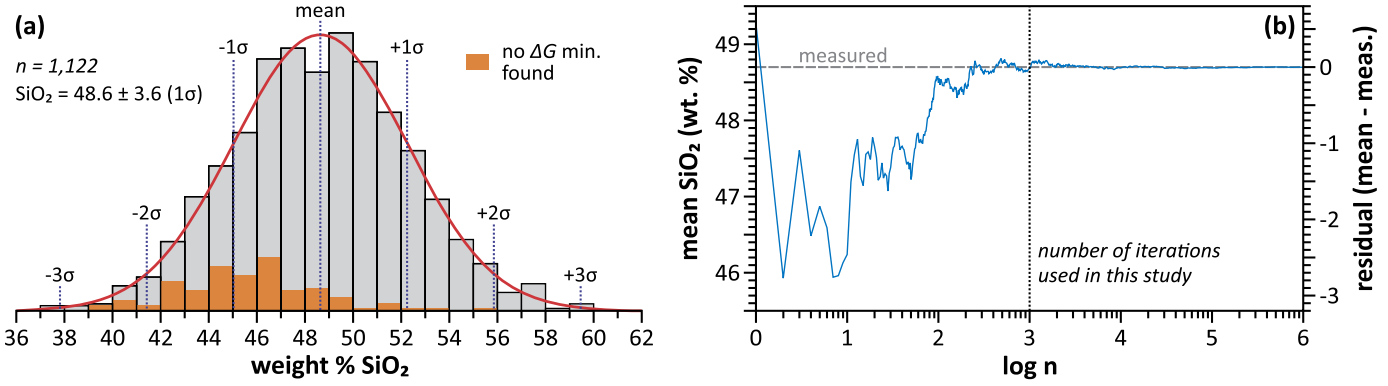

Fig. 2. (a) Example of random sampling across a normal distribution for SiO_2, with resultant confidence intervals. Simulated chemistries where free energy minimizations could not be achieved were culled and removed from considerations (orange bars). (b) Calculated mean SiO_2 through random sampling depending on the number of iterations used (n). A minimum of 1,000 iterations was used in this study because the mean falls continuously within ±0.1 wt.% of the asymptote, suggesting nominal improvements with additional iterations. (For interpretation of the colors in the figure(s), the reader is referred to the web version of this article.)

next sequential simulated bulk composition is then entered and the process was repeated until 1,000 iterations were completed.

All solution models used in PELE assume ideal mixing. Whereas this is an oversimplification, it shortened the computational time and allowed for more iterations to be computed. This also resulted in ΔG convergence issues less frequently, allowing more chemistries to be run through completion. Application of more sophisticated, non-ideal solution models would better represent the petrogenesis of the system, however would require far more computation time. To test the effects of this simplification, we have performed one calculation on the measured Venera 14 composition in MELTS_Excel (Gualda and Ghiorso, 2014) using the rhyolite-MELTS v.1.0.x calibration (Gualda et al., 2012), which is adapted with more sophisticated solution models for the mineral and melt phases (e.g., Ghiorso, 2004).

We additionally calculated enthalpy (H) to assess the responsiveness of the system to perturbations in the internal heat, such as those from radiative heat loss or latent heat of fusion. We calculated enthalpy as a function of lava crystallinity and temperature using equation (1) in Caricchi and Blundy (2015a), with the constant heat capacity (solid and melt) and heat of fusion parameters presented by Caricchi and Blundy (2015b). Enthalpy calculations are taken relative to our starting model temperature of 1350 °C.

Rheology of the crystal-bearing melt (η_{app}) is calculated using the semi-empirical parameterization of Caricchi et al. (2007), which accounts for the complex non-Newtonian behavior of crystal-bearing systems (applicable for crystal fractions between 0–0.8). Calculations use crystal fraction (Φ) and melt viscosity (η_{melt}) determined through thermodynamic modeling in PELE, with an assumed fixed strain rate of 10^{-6} s^{-1}. Note that faster strain rates will decrease the calculated η_{app} (<1 order of magnitude decrease in η_{app} for each order of magnitude increase in strain rate at 950 °C; Fig. 3c). Viscosity calculations are conducted for each iteration, with mean and 1σ standard deviation envelope calculated for the entire population.

4. Results

Thermodynamic modeling of the Venera 14 bulk rock composition places the liquidus at ~1270 °C with the onset of spinel crystallization (Fig. 3a). The relatively low mass fraction of spinel has a negligible effect on the bulk system, where melt density is only slightly decreased (<100 kg m^{-3}; Fig. 3b) and viscosity is unaffected (log η_{melt} = log η_{app} = 2.05 Pa s; Fig. 3c). Density change for the bulk system across the temperature window is the result of thermal expansivity and evolving mineral-melt proportions. Plagioclase ($X_{An} = 0.75$) crystallization at 1240 °C results in a large decrease in crystal density and initiates a departure of η_{app} from η_{melt}. There is an apparent, albeit counter-intuitive, abrupt decrease in crystal density with the onset of olivine crystallization at ~1212 °C ($X_{Fo} = 0.85$), however this is an artifact of a synchronous increase in plagioclase crystallization. The crystallization sequence to this point has only a minor effect on η_{app}, where a gradual offset from η_{melt} is observed as a result of continued increase in crystal fraction (Φ). However, subsequent crystallization of Ca-rich augite at 1154 °C and Ca-poor pigeonite at 1136 °C results in an abrupt viscosity increase, where η_{app} is increased by ~5.5 log units over this ~20 °C window. Olivine resorption shortly follows pyroxene crystallization (~1100 °C), followed by continued crystallization of spinel, plagioclase, and pyroxene for the remainder of the modeled window. Crystal fraction exceeds 0.9 by 1088 °C, at which point the residual liquid is siliceous (SiO_2 = 63.5 wt.%). Final log η_{melt} = 9.33 Pa s and log η_{app} = 18.43 Pa s (Fig. 3c). Faster strain rates of 10^{-4} and 10^{-2} s^{-1} result in calculated log η_{app} of 16.85 and 14.94 Pa s, respectively (Fig. 3c).

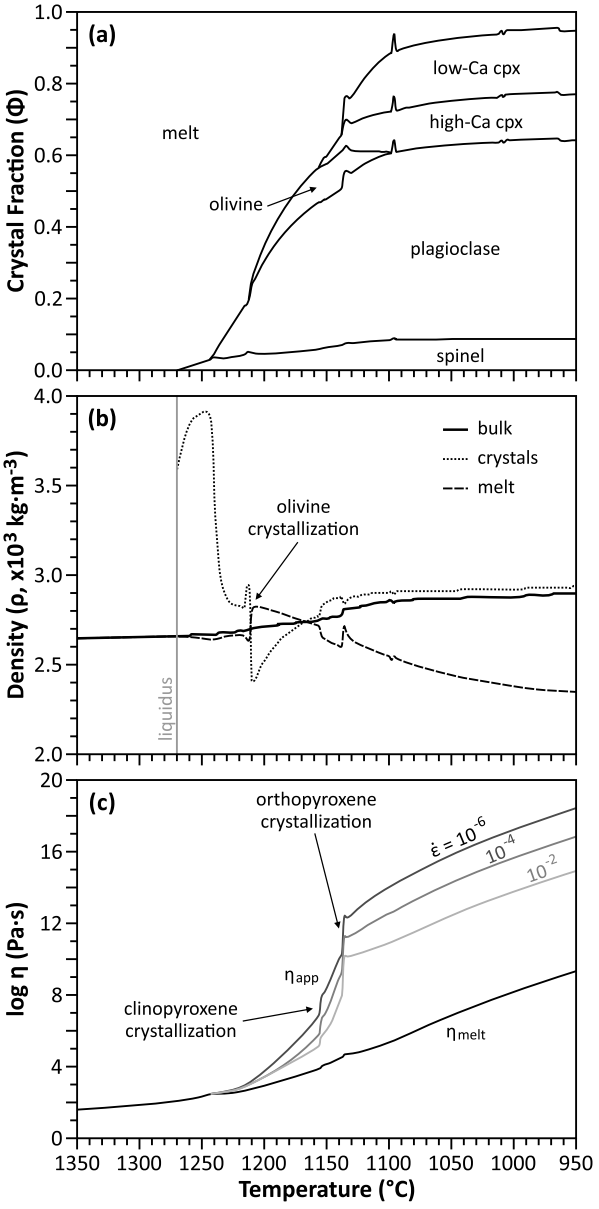

Fig. 3. Thermodynamic and rheological modeling of the Venera 14 surface chemistry. (a) Phenocryst mass fraction as a function of temperature. (b) Density of the bulk system, crystals and melt with temperature. (c) Calculated melt viscosity (η_{melt}) and modeled apparent viscosity (η_{app}) as a function of temperature. Note the sharp η_{app} increase with crystallization of clinopyroxene (at ~1155 °C) and orthopyroxene (~1138 °C). Apparent viscosity is calculated for strain rates of 10^{-6}, 10^{-4} and 10^{-2} s^{-1}, using the non-Newtonian crystal-melt viscosity model of Caricchi et al. (2007).

Modeling mineral-melt equilibria in the program MELTS_Excel, with non-ideal solution models, results in a crystallization sequence with broad similarities to that produced in PELE using only ideal mixing solutions. Whereas spinel crystallization is delayed until the lava reached cooler temperatures (~1130 °C), the onset of plagioclase and olivine crystallization and their respective compositions are largely identical; plagioclase is predicted at 1222 °C with $X_{An} = 0.79$ and olivine is predicted at 1210 °C with $X_{Fo} = 0.85$. Olivine is not completely resorbed into the melt, rather, it is only stable in trace amounts (<1.5% by weight) below 1128 °C. Whereas MELTS predicts complete crystallization of the lava below ~1080 °C, the final mineral proportions are very similar to those calculated with PELE. PELE predicts a final rock with 59% plagioclase, 33% pyroxene, and 8% spinel at 950 °C, whereas MELTS pre-

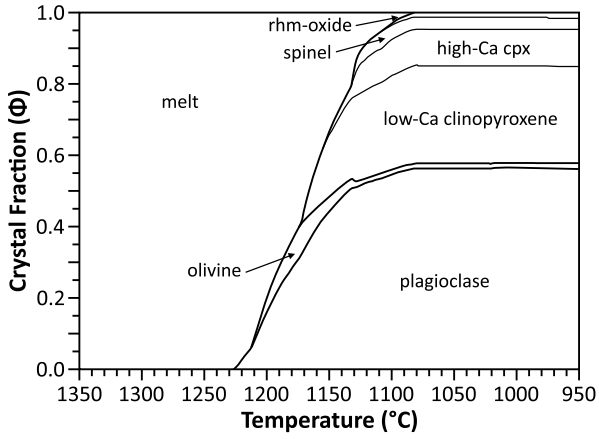

Fig. 4. Resultant mineral-melt equilibria of lava solidification of the Venera 14 surface chemistry in MELTS_Excel. Rhombohedral oxide (Rhm-oxide).

dicts an equilibrium assemblage of 57% plagioclase, 37% pyroxene, 5% oxide (spinel and titanomagnetite), and <2% olivine (Fig. 4). The evolution of Φ with cooling is also nearly identical between the two thermodynamic calculation approaches (Fig. 5d), although increases over a slightly reduced T window in MELTS.

Thermodynamic modeling in PELE was iterated for 1,000 simulated bulk compositions within the uncertainty bounds of the measured Venera 14 chemistry. The exact mineral-melt equilibria are dependent on the starting composition used, and given the large analytical uncertainty, the crystallization sequence is variable across the 1,000 iterative runs (see distribution of mineral fractions and composition in Fig. S4 of the *Auxiliary Material*). Despite this significant analytical uncertainty, lava viscosity is tightly constrained. Mean log η_{melt} increases from 1.65 ± 0.46 Pa s at 1350 °C to 8.57 ± 1.42 Pa s at 950 °C; uncertainty is consistent above ~1100 °C and only increases in the last ~100–150 °C of the modeled T-window (Fig. 5a, c). The majority of models predicted crystallization by ~1250 °C, with rapid crystal fraction increase through ~1100 °C (Fig. 5b, d). A small ($n = 59$, or 5.9% of all iterations) sub-population of low-η_{melt} models is observed at lower T, where log $\eta_{melt} < 5.0$ at 950 °C (Fig. 5a). Because this sub-set consists of <6% of the total number of iterations, the mean η_{melt} is only nominally affected and therefore does not greatly impact the uncertainty envelope.

Resultant enthalpy calculations for the Venera 14 lander geochemistry show a near-linear correlation between T and dH, with only a nominal break due to the onset of crystallization at ~1250 °C (Fig. 6a). Whereas the Φ-dH relationship is more sinuous in nature, the majority of the trend is also nearly linear (for Φ between 0.1 and 0.8). The modeling results from the measured geochemistry is statistically indistinguishable from the mean of the simulated compositions resulting from the Monte Carlo approach, except for those at high crystal fractions ($\Phi > 0.8$), however this is inconsequential because these high crystal fractions likely represent a stalled flow and exceed the applicable fractions for the apparent viscosity model. Where dΦ/dH is calculated, the measured composition results in several peaks and troughs, whereas the mean trend for the simulated compositions is relatively smooth until high crystal fractions (Fig. 6b).

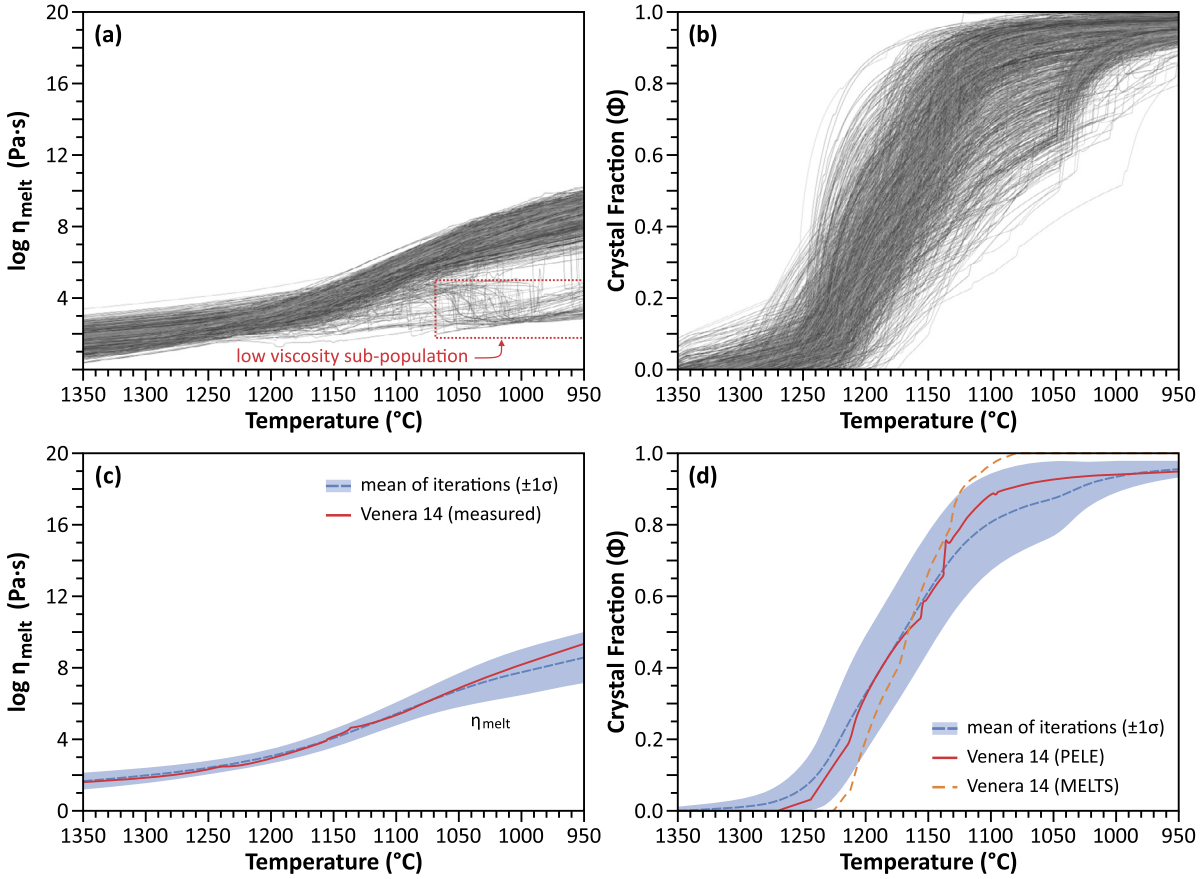

Fig. 5. Thermodynamic calculation results for geochemical uncertainty through a Monte Carlo method. (a) Calculated melt viscosity and (b) predicted crystal mass fraction (Φ) through 1,000 iterations of simulated bulk rock chemistry for the Venera 14 data. The low-viscosity sub-population discussed in this paper is shown for reference. (c) Resultant mean and 1σ uncertainty envelope across all iterations for η_{melt} and (d) crystal fraction (Φ). Modeling results for the measured composition of Venera 14 is shown for reference (red line). (For interpretation of the colors in the figure(s), the reader is referred to the web version of this article.)

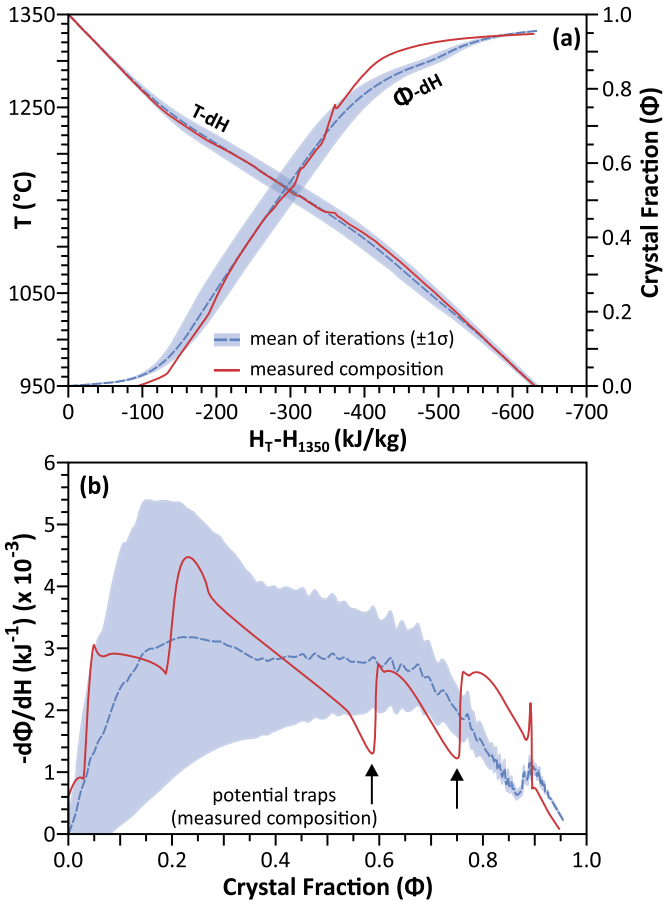

Fig. 6. Enthalpy constraints for thermodynamic equilibrium solidification modeling. (a) Temperature and crystal fraction (Φ) versus enthalpy relative to the 1350 °C starting reference state. Note the linear trends during most of crystallization (Φ between 0.1 and 0.8). (b) dΦ/dH with increasing solidification of the system. Large fluctuations are predicted for the measured composition, however these anomalies are smoothed where considering the mean of the entire simulated population.

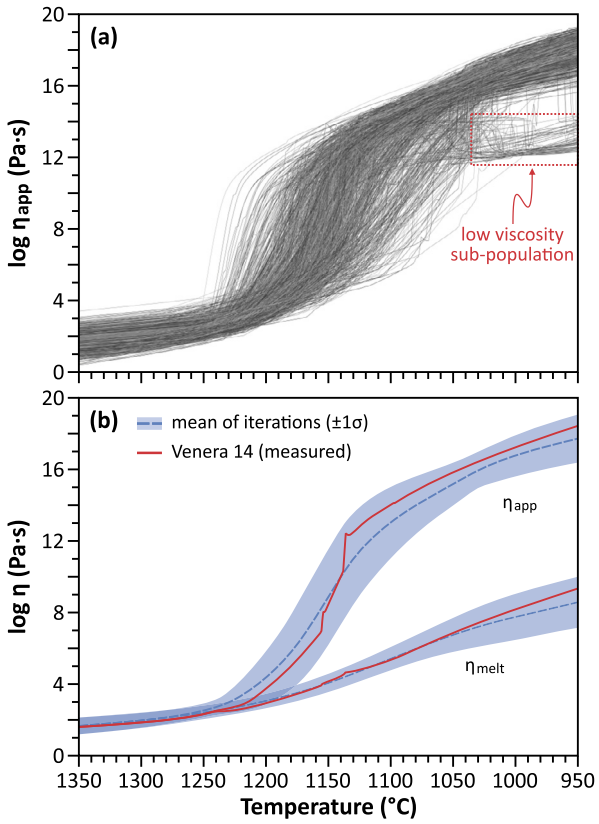

Fig. 7. (a) Calculated η_{app} from the data presented in Fig. 5, and (b) resultant mean and 1σ uncertainty envelope. Despite the very large analytical uncertainty, rheology may still be adequately constrained for the modeled flows. The low-viscosity sub-population discussed in this paper is shown in (a) for reference.

For each model iteration, the resultant η_{melt} and Φ is used to calculate η_{app} (Fig. 7a). Mean log η_{app} is statistically indistinguishable from mean log η_{melt} at temperatures >1200 °C. Cooling from 1200 °C to 1100 °C results in a rapid increase in log η_{app}, from 4.36 ± 1.49 Pa s to 13.0 ± 2.0 Pa s (Fig. 7b). Increase in log η_{app} below this temperature is more gradual through the remainder of the modeled temperature window, reaching 17.7 ± 1.3 Pa s at 950 °C. The effects of the low-η_{melt} sub-population are observed in the calculated η_{app}, where the sub-set is offset from the majority of iterations by ∼5 orders of magnitude (Fig. 7a). However, the small sampling sub-set does not greatly impact the average apparent viscosity and uncertainty envelope.

5. Discussion

5.1. Venusian flow dynamics

Various mechanisms have been proposed to explain the extensive lava flows observed on Venus. Ultramafic flow compositions have been hypothesized that would result in lower viscosity with effusion rates similar to Earth (Kargel et al., 1993; Lancaster et al., 1995). The flows observed around Panina Patera are not the longest flows found on Venus, however individual flows extending 100's of km are observed. As previously discussed, there is significant evidence that volcanism proximal to the Venera 14 landing site is the result of extension in a rift environment. Depth and mantle potential temperature does *not* suggest mantle-plume-derived melt (Lee et al., 2009; Shellnutt, 2016). Therefore, the flows present around Panina Patera cannot be explained by ultramafic compositions or exceedingly low melt viscosities. Another proposed cause of long flow lengths is due to the presence of a dense and hot CO_2-rich atmosphere. Snyder (2002) recognized that the significant absorption of CO_2 in the infrared part of the electromagnetic spectrum could suppress convection and radiant heat loss.

The modeling we present here supports the need of slow cooling rates. At higher temperature (>1200 °C), melt and apparent viscosities are relatively unchanged. However, the majority of lava solidification occurs from 1200–1100 °C, with very high crystal fractions at cooler temperatures (Fig. 5d). Near linear T-dH and Φ-dH trends across this temperature window suggests that the temperature decrease occurs as a result of equal amounts of energy removed from the system, and therefore, the relative timescale of solidification is nearly constant through this window (Fig. 6a; cf., Hartung et al., 2019). That is, there is no unique temperature window that takes significantly more heat loss to continue cooling and crystallization. Rapid increase in crystal fraction through this small temperature window results in the large increase in η_{app}, subsequently slowing the flow of lava. Pyroxene crystallization appears to drive the sharpest increase in η_{app} (+5.5 log units over ∼20 °C; Fig. 3c). Slow cooling through this window is essential as to not impede or stall the flow. Whereas dΦ/dH calculations for the measured composition results in large swings, these become reduced where considering the average of simulated compositions along the uncertainty bounds of the Venera 14 lander data (Fig. 6b). Therefore, unlike the findings from Caricchi and Blundy (2015b), there are no clear petrologic traps where the

system would tend towards a steady state regardless of enthalpic perturbations.

Modeling in MELTS_Excel, using non-ideal mixing models, results in a crystallization sequence similar to that modeled in PELE, although crystallization starts at slightly cooler temperatures (~1230 °C) and is completely crystallized by ~1080 °C. This slightly shrinks the window where crystal fraction substantially increases and furthers the need for slow cooling through this window (Fig. 5d). Use of faster strain rates has no effect on the temperatures at which this viscosity increase occurs, rather, they only affect the magnitude of viscosity increase (Fig. 3c). The lower estimate of eruption temperature for the Venera 14 volcanics by Shellnutt (2016) is ~1240 °C. If this is true, then the majority of the flow would occur within the T-window of rapid Φ increase. However, there is significant variability in the estimated eruption temperature and it is possible that the eruption occurred at higher temperatures (up to ~1350 °C). It is unlikely for any significant lava flow to have occurred below ~1100 °C because of the high crystal fraction and coupled high viscosity. Suppressed convection and radiative heat loss due to the dense CO_2 atmosphere likely aids in the slow cooling rates required to produce the flow lengths observed. Future work will utilize our petrologic and rheologic results to develop kinematic flow models to elucidate flow rates, timescales of flow emplacement, and effusion volumes to further understand Venusian igneous processes and planetary resurfacing.

A consequence of the required slow cooling rate and lava solidification is an expected increase in mineral grain sizes. The apparent viscosity model considered here does not implicitly account for crystal shape, size, and distribution, and therefore if cooling is sufficiently slow, other models that consider particle shape and size may need to be considered (e.g., Mueller et al., 2010; Mader et al., 2013). However, without hand samples and petrographic thin sections of rocks from the Venusian surface, such models are not warranted. The two-phase rheologic model we employ here is assumed to be sufficient.

5.2. Insights from a Monte Carlo approach

Application of a Monte Carlo method to assess the effects of large geochemical uncertainty on thermodynamic and rheologic modeling resulted in several discoveries. First, the large uncertainty on each oxide component may lead to simulated bulk rock chemistries that are not permissible as a result of the thermodynamic calculations failing to converge on a minimized free energy. This resulted in the removal of a non-negligible amount of iterations, typically with lower silica contents (Fig. 2a). Despite this shortcoming, the majority of iterations were able to converge on a thermodynamic solution across the modeled window. The obvious consequence of removing compositions primarily silica-poor is that the resultant melt (and therefore apparent) viscosity will be slightly skewed towards higher viscosity values. Note, however, that the mean and standard deviation of the simulated bulk rock chemistry after removal of these failed calculations are nearly identical and statistically indistinguishable from the measured Venera 14 chemistry (Table 1).

The second finding from this approach is that despite the large variability in compositions, the resultant models were remarkably consistent, particularly with respect to η_{melt}. The development of Gaussian probabilistic distributions to randomly sample for each oxide component means that in some instances (only a couple of iterations over the >1,000 simulated compositions), random sampling was done beyond a 3σ confidence interval. This can have a drastic effect on the range of oxide concentrations for certain components. For example, silica has individual runs sampling from ~37 to 60 wt.% and MgO ranges from <1 to 19 wt.%. However, the mean and standard deviation from all iterative runs were tightly constrained, typically within approximately ± 1 log unit for η_{melt} across the temperature window (within ± 0.5 log units at higher temperatures; Fig. 5c). Different crystallization sequences resulting from the variable chemistries resulted in Φ–T pathways that are more diffuse, however uncertainty envelopes are still informative and lead to well-confined η_{app} values. For instance, a large increase in crystal fraction is observed between 1200 and 1100 °C (Fig. 5d). This significant crystallization event drives a large increase in apparent viscosity, suggesting large perturbations in lava rheology for this ~100 °C window can be expected (Fig. 7b). We note, however, that the thermodynamic and rheological modeling approaches used in this study are best suited for compositions similar to those used in the experiments in which the respective models are based. Caution should be used where interpreting data derived from compositions greatly extrapolated outside of these compositional bounds, and may contribute to the consistency of our results despite the significant analytical uncertainty.

Finally, the increased uncertainty in η_{melt} and η_{app} at lower T is the result of different mineral-melt equilibria schemes affecting the residual melt composition, in particular due to the presence of the low-η_{melt} sub-population (Fig. 5a). Statistical analysis of variance (ANOVA) and post-hoc Tukey test of the compositional differences between the majority of iterations versus this sub-population shows that this sub-set consists of low-Si ($SiO_2 = 44.36$ wt.%) bulk compositions. This would result in silica-poor melt and lower viscosities (see *Auxiliary Material* for more detail; Figs. S2 and S3). The apparent effects of this offset on calculated η_{app} are significant, with a departure of ~5 orders of magnitude between this sub-population and the majority of compositions modeled (Fig. 5b). However, because so few of the total runs (<6%) comprise this sub-population, the mean viscosity is not greatly impacted.

6. Conclusions

Our understanding of Venusian igneous processes, lava flow volumes, and effusion rates are dependent upon being able to constrain solidification sequences and evolving flow rheology. With no known meteorite samples from Venus, we are reliant upon the very limited surface data of the bulk rock geochemistry from the Venera and Vega landers to constrain these parameters. The significant analytical uncertainties with these measurements make assessing the effects of said uncertainty on thermodynamic and rheologic modeling results challenging. Through application of a Monte Carlo method, we are able to determine mineral-melt equilibria, crystal fraction, melt viscosity and apparent viscosity from 1350 °C to 950 °C, and develop statistical uncertainty envelopes for these parameters. We show that despite the limited geochemical data and large analytical uncertainties, petrologic and rheologic evolution of lava solidification can be reasonably estimated and statistically bounded by uncertainty envelopes. These results provide an important starting constraint for future modeling of individual lava flow dynamics with a goal of estimating effusion rates and flow volumes.

Acknowledgements

We thank James Thompson for helpful discussions and Brittany Ashley for assistance in dataset management, coding and data parsing. This manuscript was greatly improved through reviewer feedback by Luca Caricchi, a second anonymous reviewer, and by handling editor Tamsin Mather. This work is supported by NSF-EAR grant #1524011 and NASA grant #NMO710630 (project #405129), both awarded to M.S. Ramsey.

Appendix A. Supplementary material

Supplementary material related to this article can be found online at https://doi.org/10.1016/j.epsl.2019.03.036.

References

Abdrakhimov, A., 2001. Geologic mapping of Venera 14 landing site region. In: Lunar and Planetary Science Conference, 1670.

Basilevsky, A., McGill, G., 2007. Surface evolution of Venus. In: Geophysics Monograph, vol. 176, pp. 23–43.

Boudreau, A.E., 1999. PELE – a version of the MELTS software program for the PC platform. Comput. Geosci. 25, 201–203.

Bruno, B.C., Taylor, G.J., 1995. Morphologic investigation of Venusian lavas. Geophys. Res. Lett. 22, 1897–1900.

Campbell, I.H., 2007. Testing the plume theory. Chem. Geol. 241, 153–176.

Caricchi, L., Blundy, J., 2015a. The temporal evolution of chemical and physical properties of magmatic systems. In: Caricchi, L., Blundy, J.D. (Eds.), Chemical, Physical and Temporal Evolution of Magmatic Systems. Geol. Soc. (Lond.) Spec. Publ. 422, 1–15.

Caricchi, L., Blundy, J., 2015b. Experimental petrology of monotonous intermediate magmas. In: Caricchi, L., Blundy, J.D. (Eds.), Chemical, Physical and Temporal Evolution of Magmatic Systems. Geol. Soc. (Lond.) Spec. Publ. 422, 105–130.

Caricchi, L., Burlini, L., Ulmer, P., Gerya, T., Vassalli, M., Papale, P., 2007. Non-Newtonian rheology of crystal-bearing magmas and implications for magma ascent dynamics. Earth Planet. Sci. Lett. 264, 402–419.

Crumpler, L.S., Aubele, J.C., Senske, D.A., Keddie, S.T., Magee, K.P., Head, J.W., 1997. Volcanoes and ceneters of volcanism on Venus. In: Bougher, S.W., Hunten, D.M., Phillips, R.J. (Eds.), Venus II: Geology, Geophysics, Atmosphere, and Solar Wind Environment. University of Arizona Press, Tucson, pp. 697–756.

Fegley Jr., B., 2004. Venus. In: Davis, A.M., Holland, H.D. (Eds.), Meteorites, Comets, and PlanetsIn: Turekian, K.K., Holland, H.D. (Eds.), Treatise on Geochemistry, vol. 1. Elsevier-Pergamon, Oxford, pp. 487–507.

Fegley Jr., B., Klingelhöfer, G., Lodders, K., Widemann, T., 1996. Geochemistry of surface-atmosphere interactions on Venus. In: Boucher, S.W., Hunten, D., Phillips, R. (Eds.), Venus II. University of Arizona Press, Tucson, AZ.

Hess, P.C., Head, J.W., 1990. Derivation of primary magmas and melting of crystal materials on Venus: some preliminary petrogenetic considerations. Earth Moon Planets 50/51, 57–80.

Gale, A., Dalton, C.A., Langmuir, C.H., Su, Y., Schilling, J.G., 2013. The mean composition of ocean ridge basalts. Geochem. Geophys. Geosyst. 14, 173–180.

Ghiorso, M.S., 1985. Chemical mass transfer in magmatic processes I. Thermodynamic relations and numerical algorithms. Contrib. Mineral. Petrol. 90, 107–120.

Ghiorso, M.S., 2004. An equation of state for silicate melts. I. Formulation of a general model. Am. J. Sci. 304, 637–678.

Ghiorso, M.S., Sack, R.O., 1995. Chemical mass transfer in magmatic processes, IV. A revised and internally consistent thermodynamic model for the interpolation and extrapolation of liquid-solid equilibria in magmatic systems at elevated temperatures and pressures. Contrib. Mineral. Petrol. 119, 197–212.

Grimm, R.E., Hess, P.C., 1997. The crust of Venus. In: Bougher, S.W., Hunten, D.M., Philips, R.J. (Eds.), Venus II. University of Arizona Press, Tucson, AZ, pp. 1205–1244.

Grindrod, P.M., Stofan, E.R., Guest, J.E., 2010. Volcanism and resurfacing on Venus at the full resolution of Magellan SAR data. Geophys. Res. Lett. 37, L15201.

Gualda, G.A.R., Ghiorso, M.S., 2014. MELTS_Excel: a Microsoft Excel-based MELTS interface for research and teaching of magma properties and evolution. Geochem. Geophys. Geosyst. 16, 315–324.

Gualda, G.A.R., Ghiorso, M.S., Lemons, R.V., Carley, T.L., 2012. Rhyolite-MELTS: a modified calibration of MELTS optimized for silica-rich, fluid-bearing magmatic systems. J. Petrol. 53, 875–890.

Hansen, V.L., Young, D.A., 2007. Venus's evolution: a synthesis. In: Cloos, M., Carlson, W.D., Gilbert, M.C., Liou, J.G., Sorensenm, S.S. (Eds.), Convergent Margin Terranes and Associated Ridges: A tribute to W.G. Ernst. Geological Society of America, pp. 255–273. Special Paper 419.

Hartung, E., Weber, G., Caricchi, L., 2019. The role of H_2O on the extraction of melt from crystallising magmas. Earth Planet. Sci. Lett. 508, 85–96.

Herzberg, C., Gazel, E., 2009. Petrologic evidence for secular cooling in mantle plumes. Nature 458, 619–622.

Herzberg, C., Asimow, P.D., Arndt, N., Niu, Y., Lesher, C.M., Fitton, J.G., Cheadle, M.J., Saunders, A.D., 2007. Temperatures in ambient mantle and plumes: constraints from basalts, picrites, and komatiites. Geochem. Geophys. Geosyst. 8 (2), Q02006.

Kargel, J.S., Komatsu, G., Baker, V.R., Strom, R.G., 1993. The volcanology of Venera and VEGA landing sites and the geochemistry of Venus. Icarus 103, 253–275.

Kaula, W.M., 1995. Venus reconsidered. Science 270, 1460–1464.

Lancaster, M.G., Guest, J.E., Magee, K.P., 1995. Great lava flow fields on Venus. Icarus 118, 69–86.

Lee, C.-T.A., Luffi, P., Plank, T., Dalton, H., Leeman, W.P., 2009. Constraints on the depths and temperatures of basaltic magma generation on Earth and other terrestrial planets using new thermobarometers for mafic magmas. Earth Planet. Sci. Lett. 279, 20–33.

Lodders, K., Fegley, J.B., 1998. The Planetary Scientist's Companion. Oxford University Press, Oxford. 371 pp.

Mackwell, S.J., Zimmerman, M.E., Kohlstedt, D.L., 1998. High-temperature deformation of dry diabase with application to tectonics on Venus. J. Geophys. Res. 103 (B1), 975–984.

Mader, H., Llewellin, E., Muller, S., 2013. The rheology of two-phase magmas: a review and analysis. Bull. Volcanol. 257, 135–158.

Magganas, A., Koutsovitis, P., 2015. Composition, melting and evolution of the upper mantle beneath the Jurassic Pindos ocean inferred by ophiolitic ultramafic rocks in East Othris, Greece. Int. J. Earth Sci. 104, 1185–1207.

Malliband, C.C., Martin, P., McCaffrey, K.J.W., Macpherson, C.G., Stofan, E.R., 2017. The geological history of Aleksota Mons, Venus. In: 48th Lunar and Planetary Science Conference. Woodlands, Texas, abstract #1395.

Mueller, S., Llewellin, E.W., Mader, H.M., 2010. The rheology of suspensions of solid particles. Philos. Trans. R. Soc. Lond. A 466, 1201–1228.

Seiff, A., Schofield, J.T., Kliore, A.J., Taylor, F.W., Limaye, S.S., Revercomb, H.E., Sromovsky, L.A., Kerzhanovich, V.I., Moroz, V.I., Marov, M.Y., 1986. Models of the structure of the atmosphere of Venus from the surface to 100 km altitude. In: Kliore, A.J., Moroz, V.I., Keating, G.M. (Eds.), The Venus International Reference Atmosphere. Pergamon, Oxford, pp. 3–58.

Shellnutt, J.G., 2016. Mantle potential temperature estimates of basalt from the surface of Venus. Icarus 277, 98–102.

Snyder, D., 2002. Cooling of lava flows on Venus: the coupling of radiative and convective heat transfer. J. Geophys. Res. 107 (E10), 5080.

Stofan, E.R., Guest, J.E., Copp, D.L., 2001. Development of large volcanoes on Venus: constraints from Sif, Gula, and Kunapipi Montes. Icarus 152, 75–95.

Surkov, Y.A., Barsukov, V.L., Moskalyeva, L.P., Kharyukova, V.P., Kemurdzhian, A.L., 1984. New data on the composition, structure, and properties of Venus rock obtained by Venera 13 and Venera 14. In: Proceedings of the 14th Lunar and Planetary Science Conference, Part 2. J. Geophys. Res. 89, B393–B402.

Surkov, Y.A., Moskalyova, L.P., Kharyukova, V.P., Dudin, A.D., Smirnov, G.G., Zaitseva, S.Y., 1986. Venus rock composition at the Vega 2 Landing Site. J. Geophys. Res., Solid Earth 91 (B13), E215–E218.

Treiman, A.H., 2007. Geochemistry of Venus surface: current limitations as future opportunities. In: Esposito, L.W., Stofan, E.R., Cravens, T.E. (Eds.), Exploring Venus as a Terrestrial Planet. In: Geophysical Monograph Series, p. 250.

Weitz, C.M., Basilevsky, A.T., 1993. Megellan observations of the Venera and Vega Landing Site regions. J. Geophys. Res. 98 (E9), 17069–17097.